Observing and Understanding Earth Rotation

Richard S. Gross

Jet Propulsion Laboratory
California Institute of Technology
Pasadena, CA 91109–8099, USA

International Summer School on Space Geodesy and Earth System

August 21–25, 2012
Shanghai, China

Earth Orientation Parameters

- Earth's orientation in space given by 5 parameters:
  - 2 precession-nutation parameters ($\Delta\psi$, $\Delta\varepsilon$)
    - Specifies location of spin axis in *celestial* reference frame
  - 2 polar motion parameters (PMX, PMY)
    - Specifies location of spin axis in *terrestrial* reference frame
  - 1 spin parameter (UT1)
    - Specifies angle through which Earth has rotated about spin axis

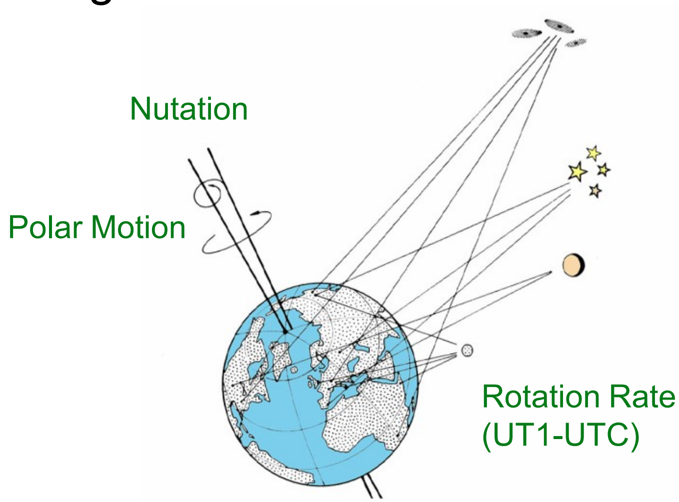

Earth Rotation Dynamics

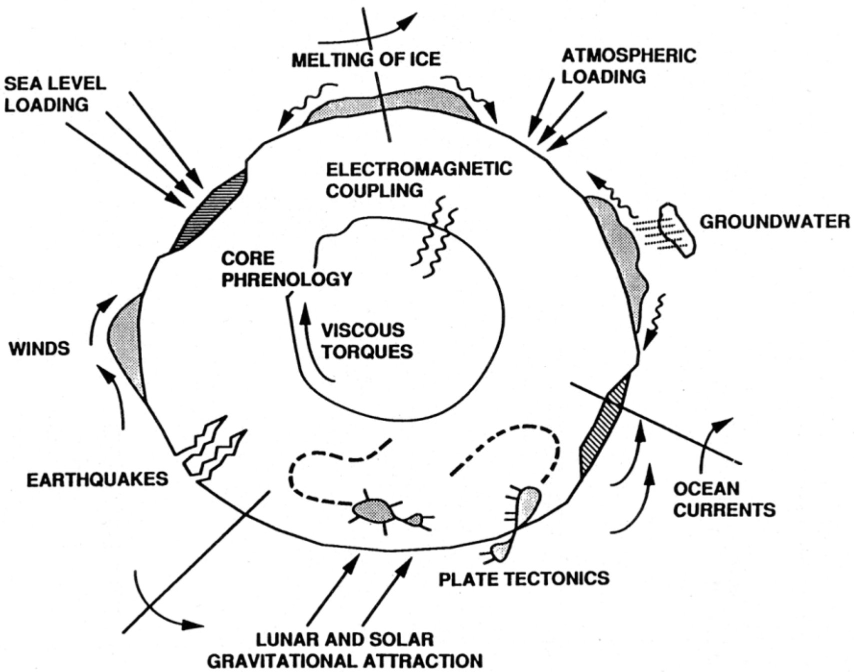

Sources of Earth Rotation Variations

Rotation of Earth changes

Length of day by few milliseconds

Wobbles by few hundred milliarcsec

(10 meters at North Pole)

Nutation and precession

Rotation changes caused by

External torques — tidal phenomena

Internal deformation — earthquakes, postglacial rebound

Angular momentum exchange with bounding fluids — atmosphere, oceans, core

Studying Earth's rotation improves knowledge of

Rheology and dissipation processes of solid Earth

Interior figure of Earth

Core-mantle coupling

A Brief History of Earth Rotation

Edmond Halley
(1656-1742)

English astronomer

In 1695 Edmond Halley noted that the Moon is apparently accelerating in its orbit

In 1939 Harold Spencer Jones conclusively demonstrated that the Earth's rotation is slowing down

In 1955 atomic clocks provide uniform timescale for determining changes in Earth's rate of rotation

Leonhard Euler
(1707-1783)

Swiss mathematician

In 1765 published *Theoria Motus Corporum Solidorum*

Predicted Earth should freely wobble as it rotates

Period of wobble: 306 days

Seth Carlo Chandler, Jr.
(1846-1913)

American astronomer

In 1891 Chandler observed the free wobble of the Earth that was predicted in 1765 by Euler

Period of observed wobble:
427 days

Later in 1891 Simon Newcomb explained difference between prediction and observation as due to “elasticity of the Earth” and “fluidity of the ocean”

Observations

Observed Earth Rotation Variations

Polar Motion
2001-2007 and
mean pole since 1900

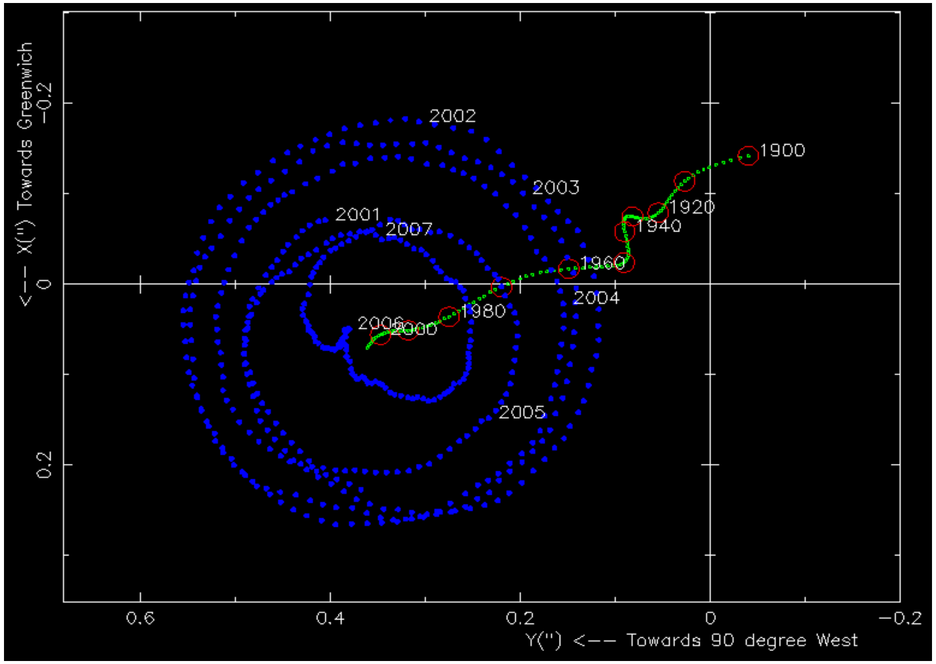

ms UT1-UTC (1/1/00-3/31/08)

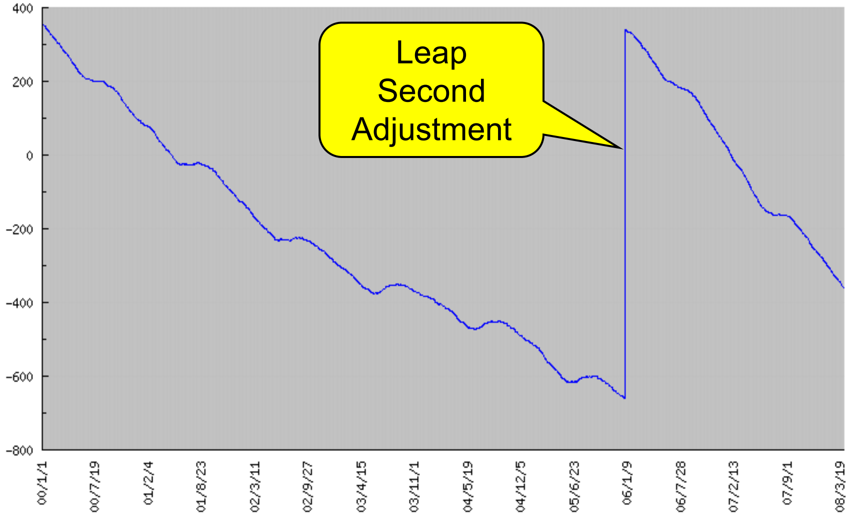

Length of Day Offset (1/1/00-3/31/08)

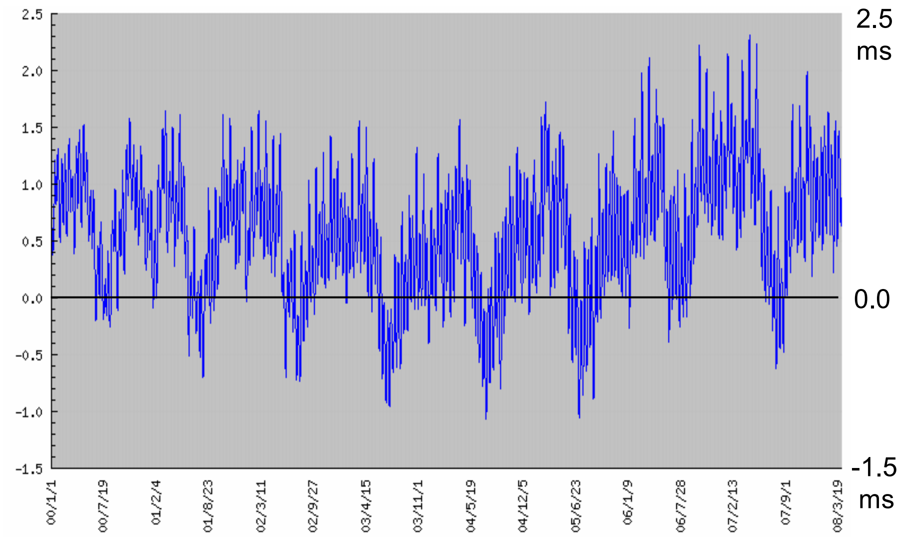

Global Navigation Satellite Systems

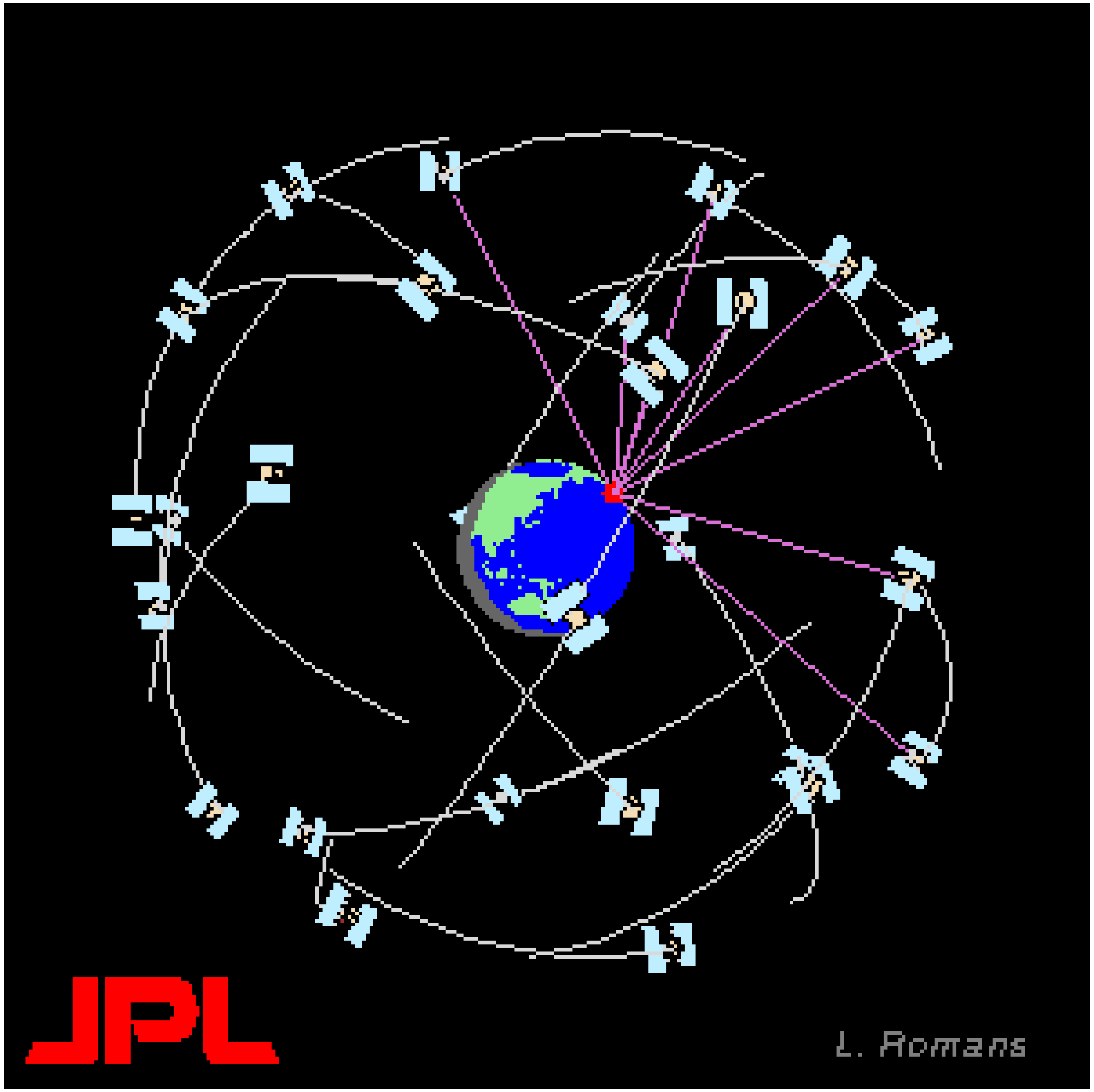

Satellite Laser Ranging

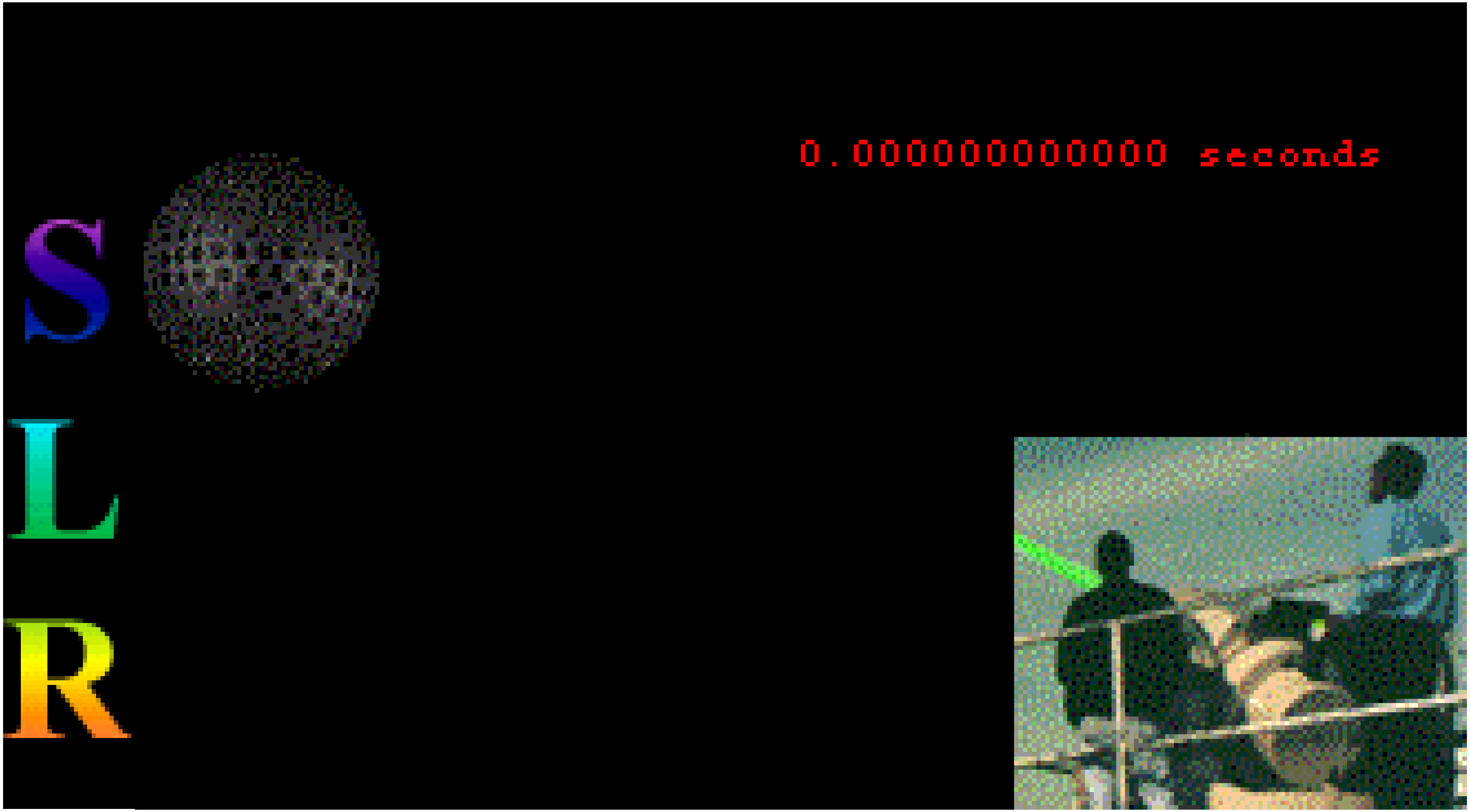

Interpretation

Mass Transport in the Earth System

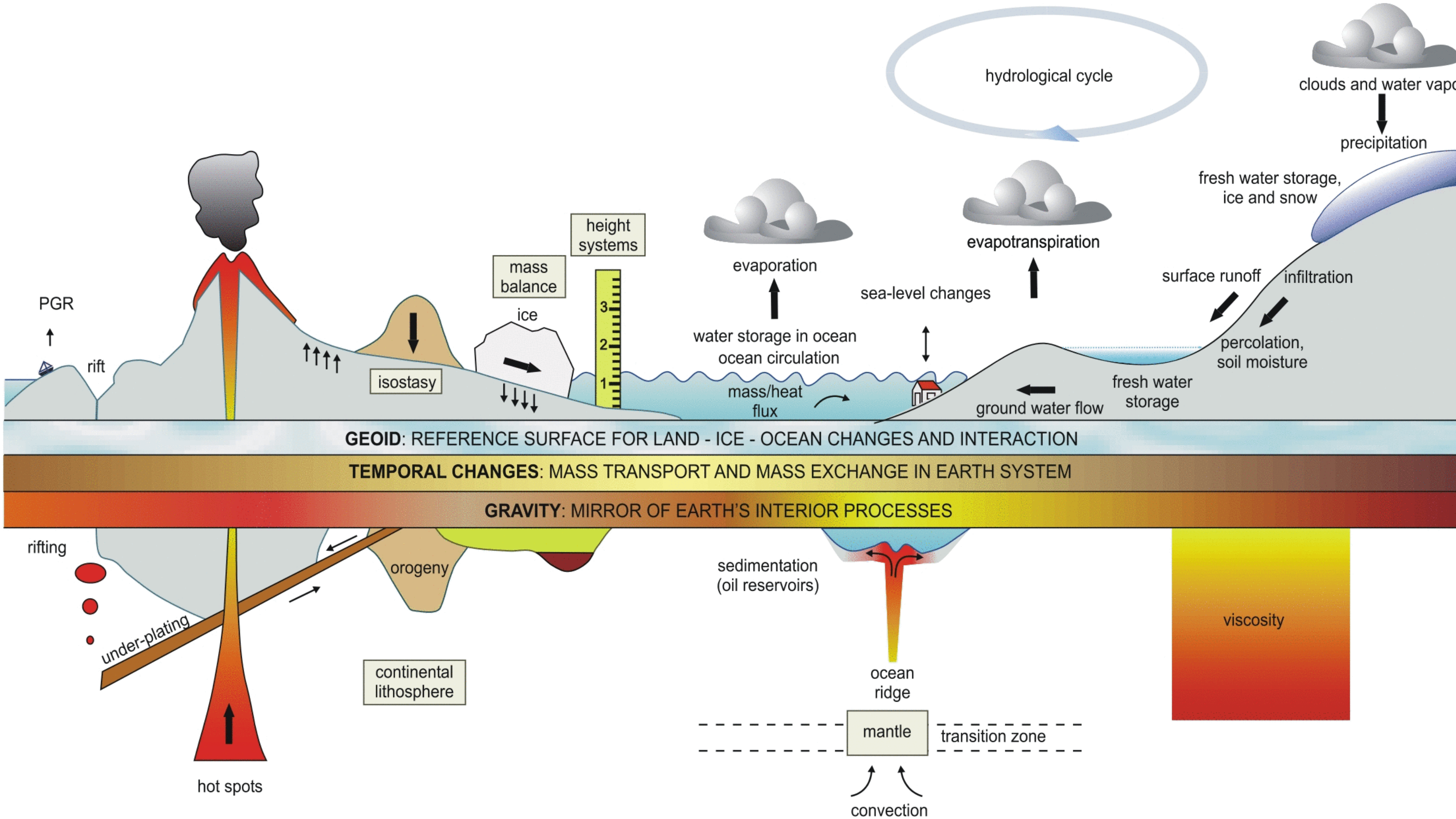

Ilk et al. (2005)

Forcing Mechanisms

- External
  - Tidal potential
    - Body, ocean, atmosphere
- Surficial
  - Atmospheric winds and surface pressure
  - Oceanic currents and bottom pressure
  - Water stored on land (liquid, snow, ice)
- Internal
  - Earthquakes and tectonic motions
  - Mantle convection
  - Outer core dynamics / coupling with mantle
  - Inner core dynamics / coupling with outer core and mantle

Geodetic Measures of Earth's Response

- Rotation
  - Angular momentum exchange (surface fluids, outer core)
  - Torques (external, surficial, internal)
  - Changes in inertia tensor (earthquakes, GIA)
- Gravity and geocenter
  - Mass distribution (static field)
  - Mass redistribution (time varying field)
  - Surface displacements (ground-based)
- Shape
  - Tidal displacements
  - Surface loading and unloading
  - Internal deformation
    - Earthquakes, core pressure => mantle deformation

Tidal Variations: Dissipation

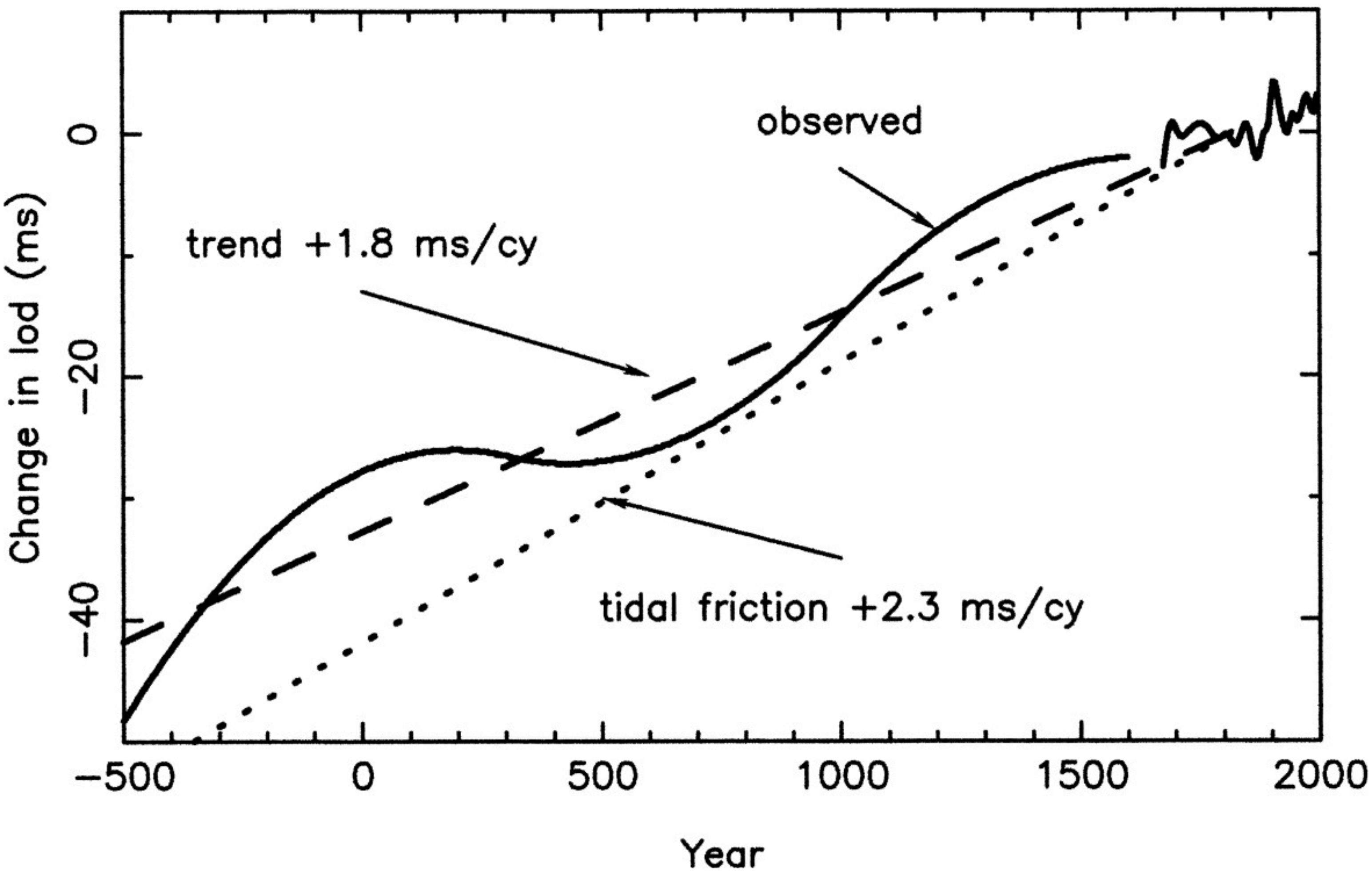

Secular change in the length-of-day during the past 2500 years estimated from lunar and solar eclipse, lunar occultation, optical astrometric, and space-geodetic observations. The difference between the observed secular trend and that caused by tidal friction is due to the effects of glacial isostatic adjustment and other processes such as ice sheet mass change and the accompanying nonsteric change in sea level. From Morrison and Stephenson (2001).

Tidal Variations: Long-Period

Observed Length-of-Day

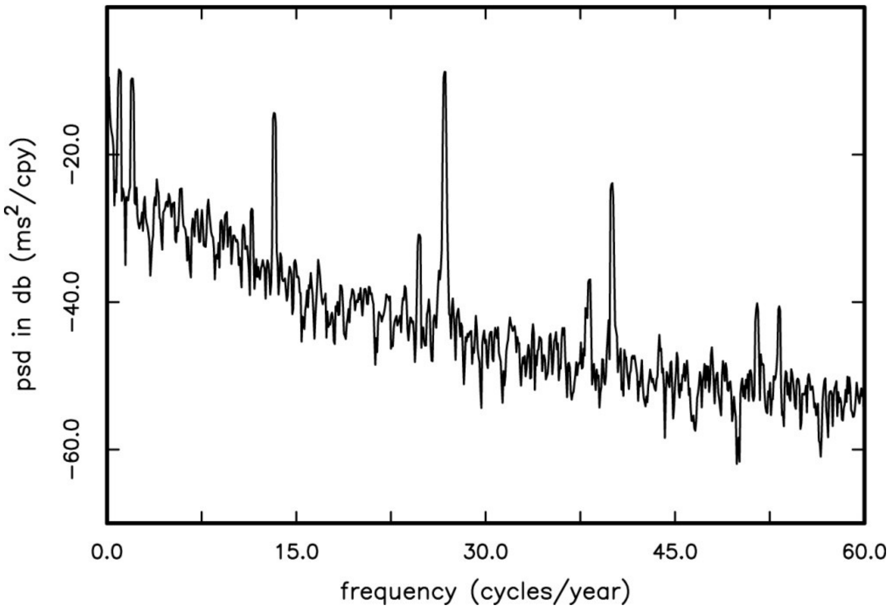

Gross (2009)

Observed Length-of-Day

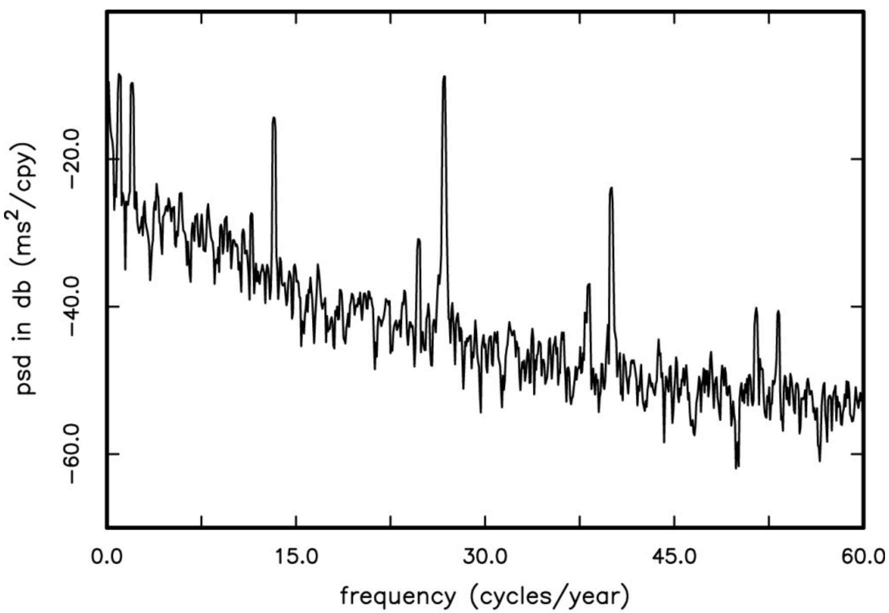

Remove AAM & OAM

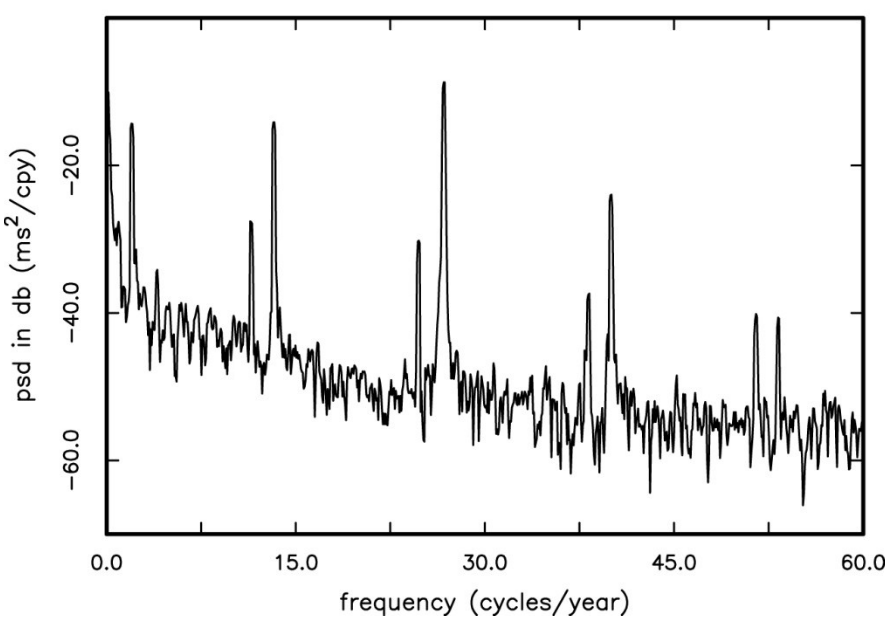

Gross (2009)

Observed Length-of-Day

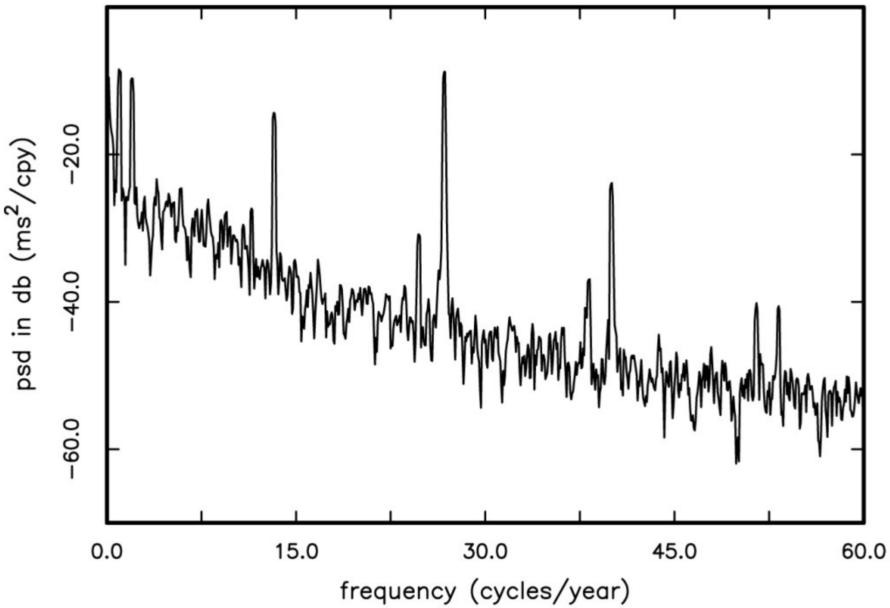

Remove AAM & OAM

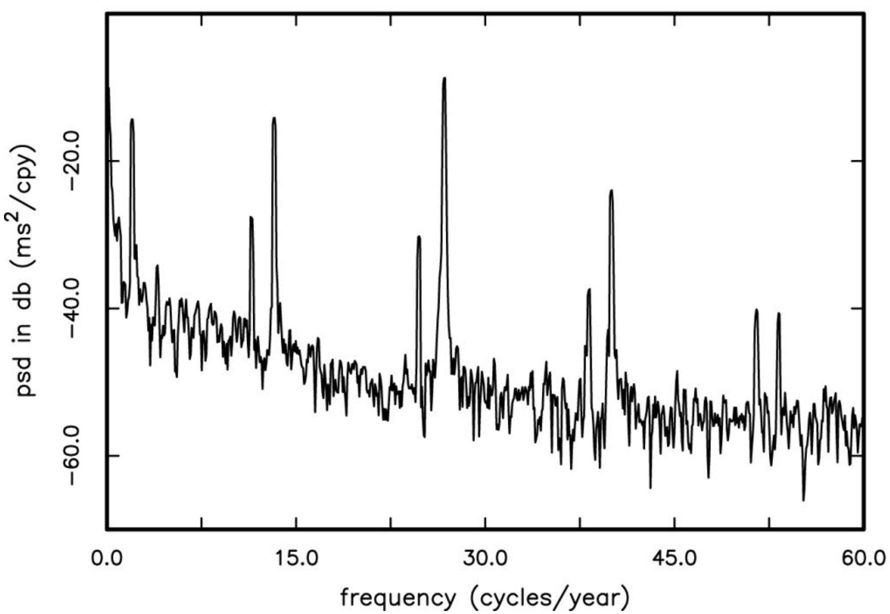

Remove Body Tides (Yoder & WB86)

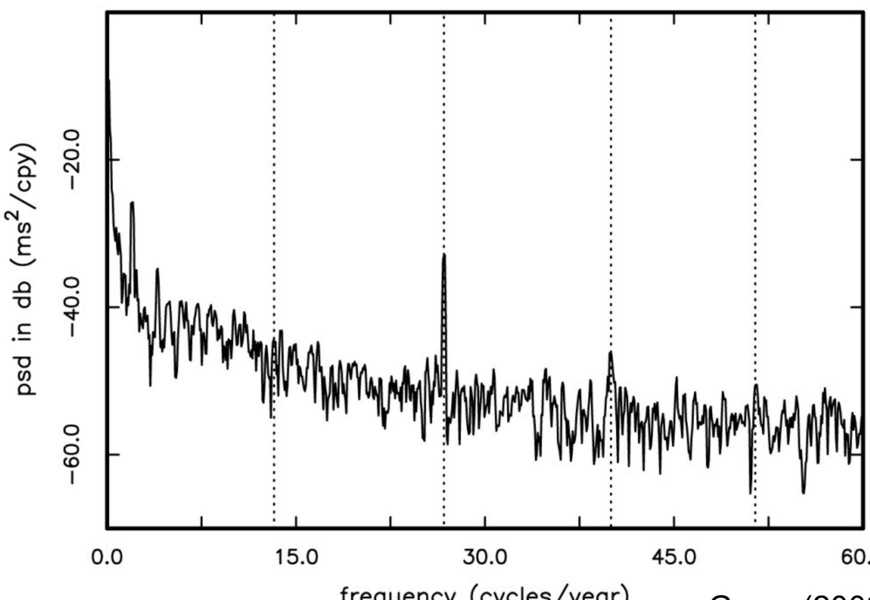

Gross (2009)

Observed Length-of-Day

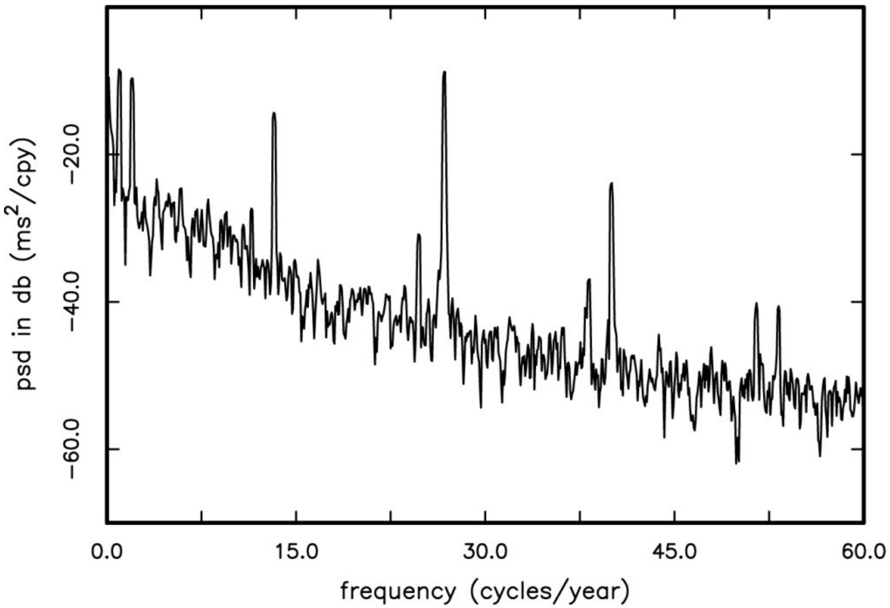

Remove Ocean Tides (KSD98)

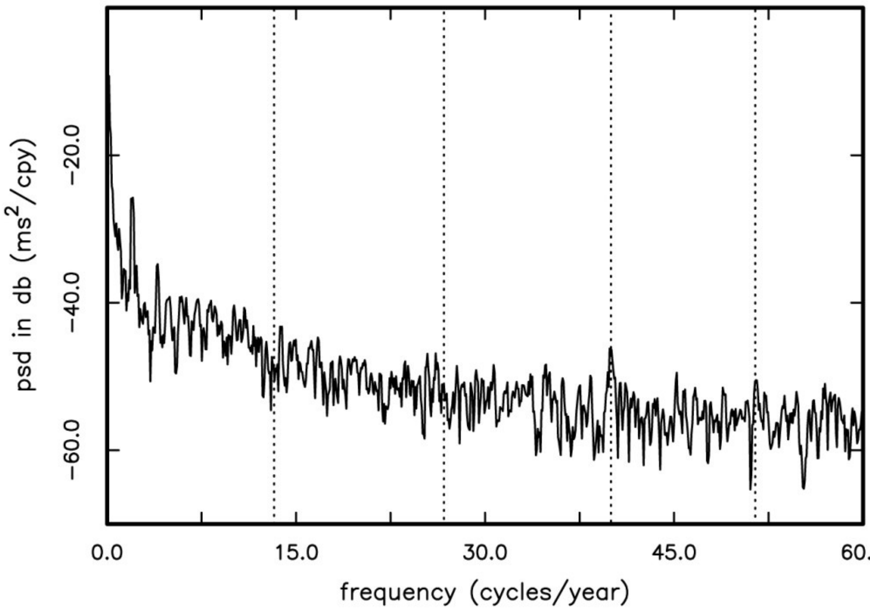

Remove AAM & OAM

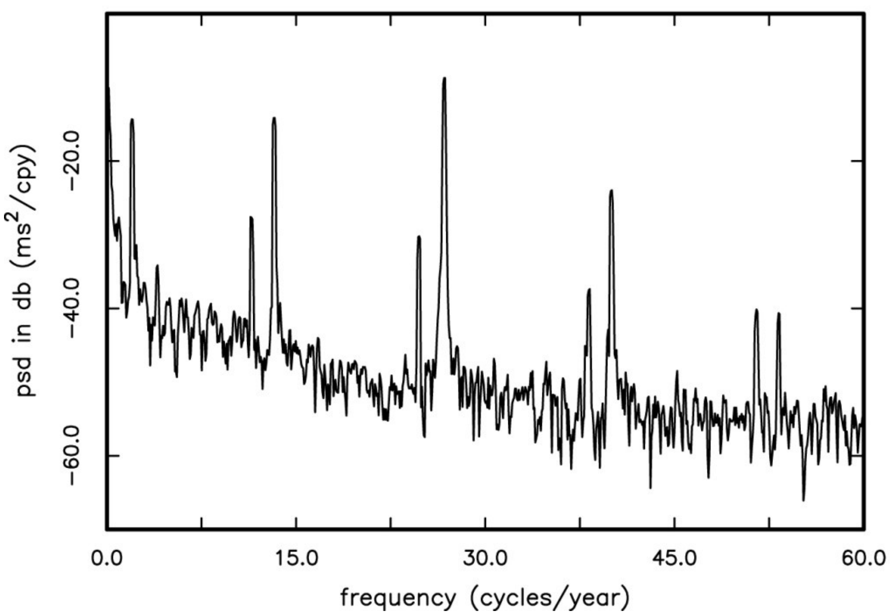

Remove Body Tides (Yoder & WB86)

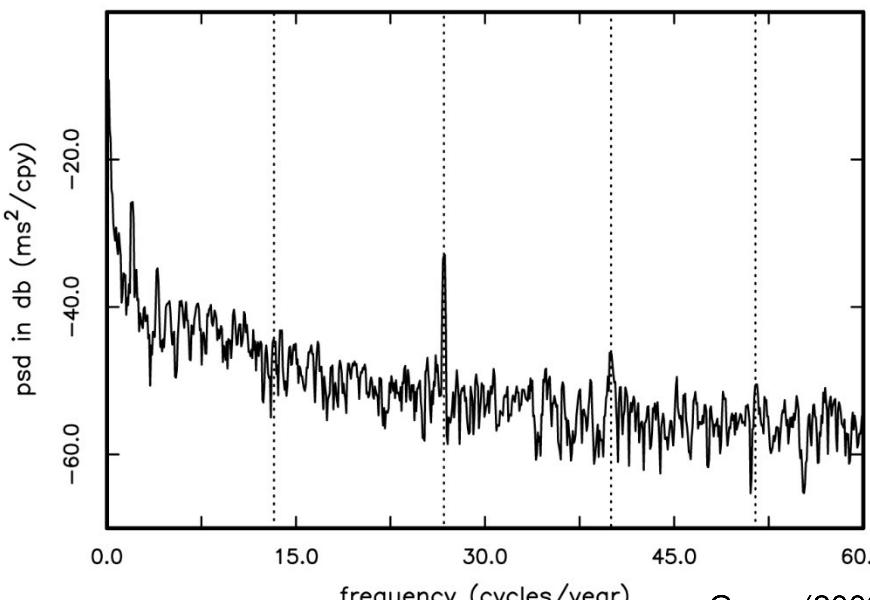

Gross (2009)

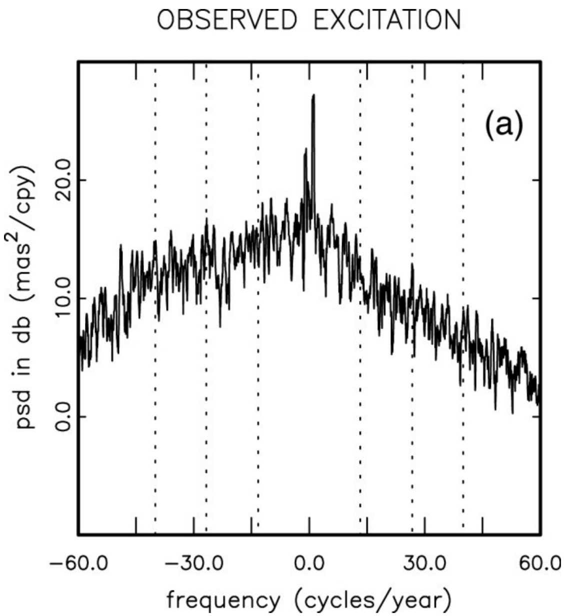
OBSERVED EXCITATION
(a)
psd in db (mas2/cpy)
20.0
10.0
0.0
−60.0
−30.0
0.0
30.0
60.0
frequency (cycles/year)

Gross (2008)

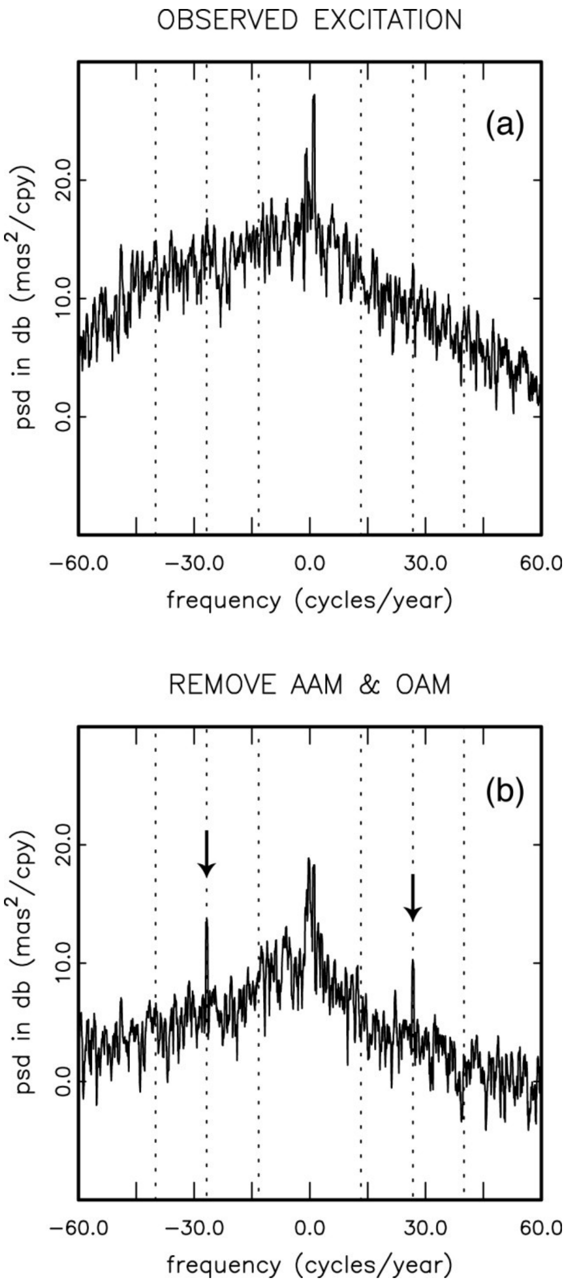
OBSERVED EXCITATION
(a)
psd in db (mas²/cpy)
20.0
10.0
0.0
−60.0
−30.0
0.0
30.0
60.0
frequency (cycles/year)
REMOVE AAM & OAM
(b)
psd in db (mas²/cpy)
20.0
10.0
0.0
−60.0
−30.0
0.0
30.0
60.0
frequency (cycles/year)

Gross (2008)

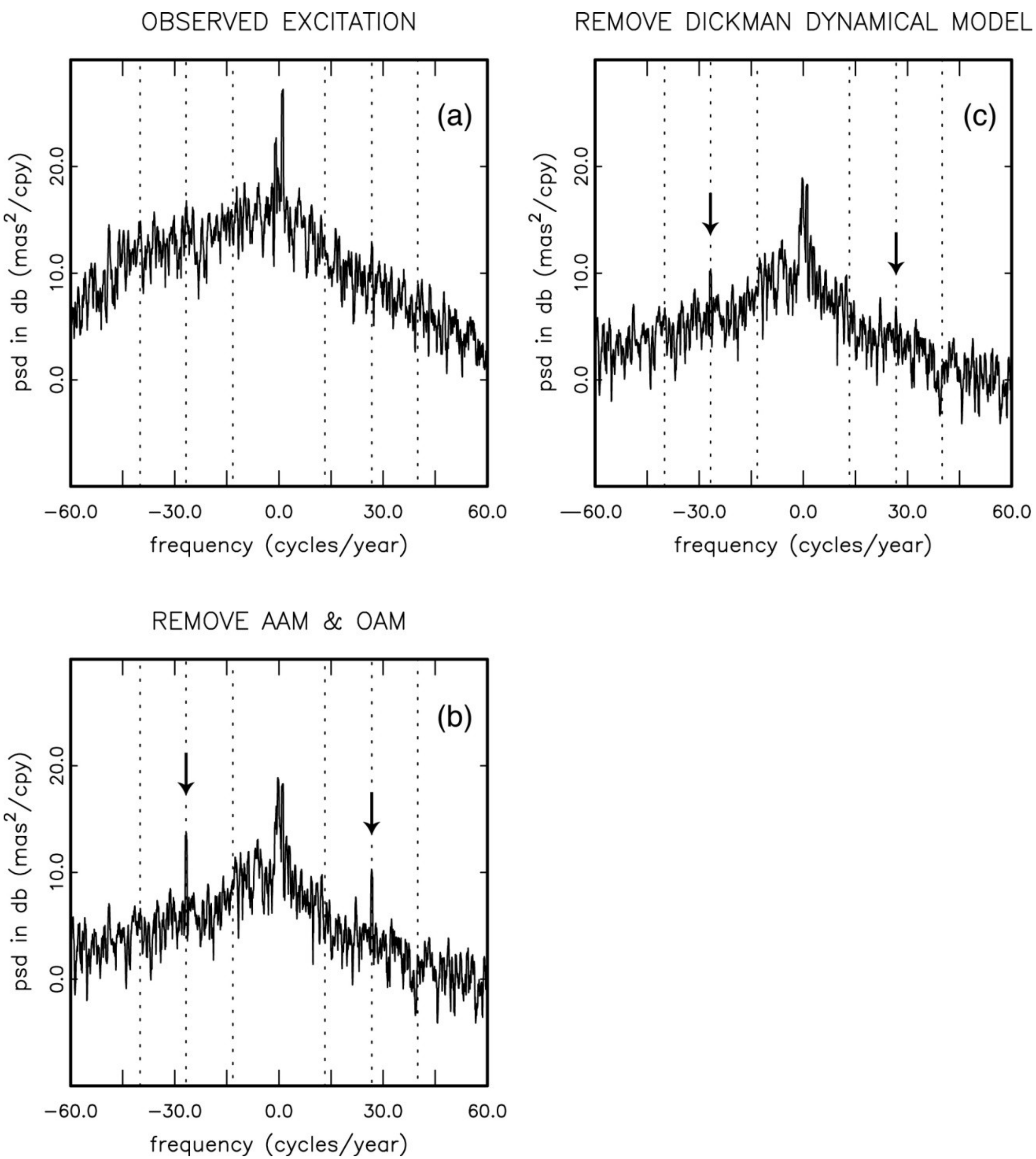
OBSERVED EXCITATION
(a)
REMOVE AAM & OAM
(b)
REMOVE DICKMAN DYNAMICAL MODEL
(c)
psd in db (mas^2/cpy)
0.0
10.0
20.0
frequency (cycles/year)
−60.0
−30.0
0.0
30.0
60.0

Gross (2008)

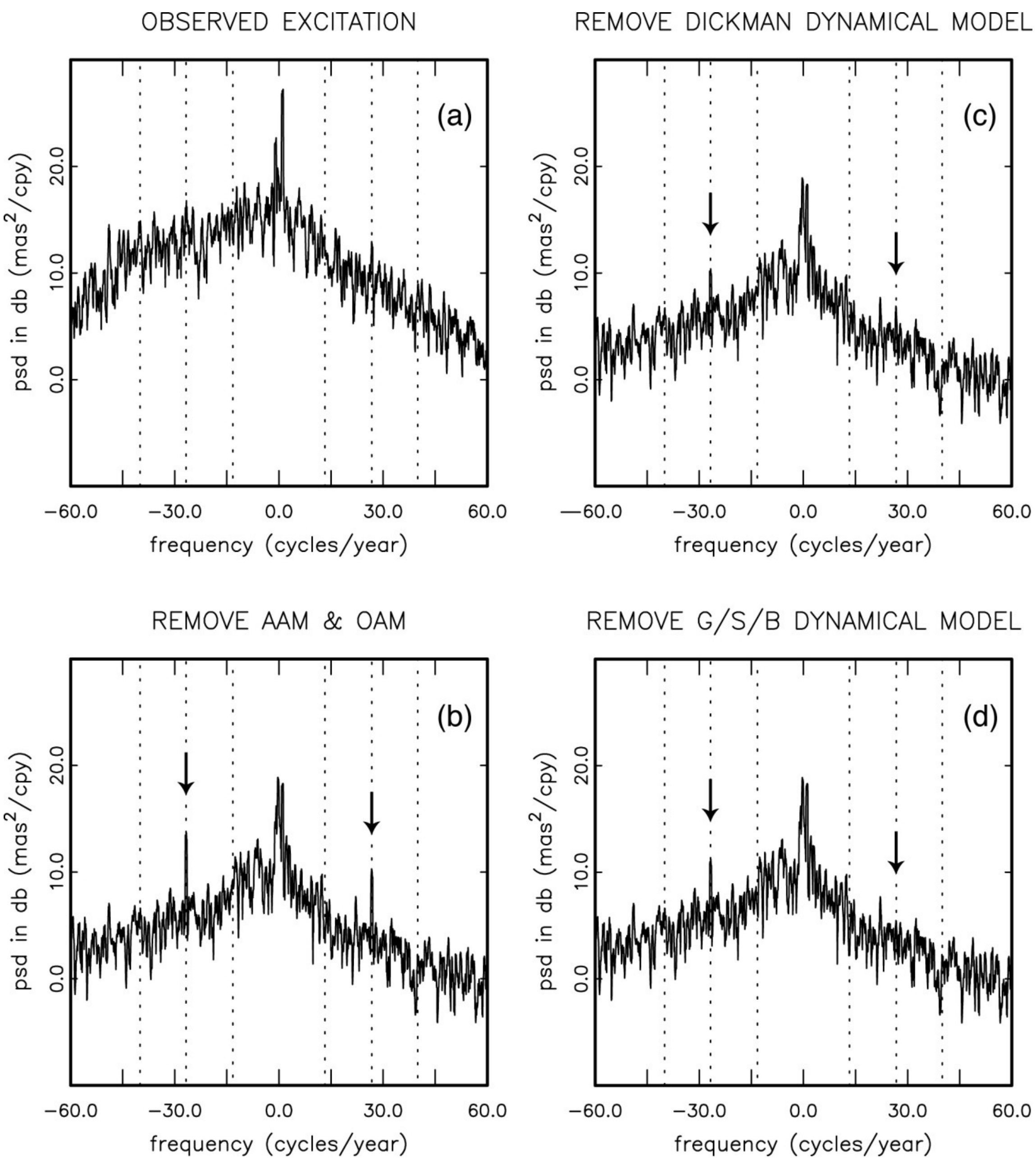
OBSERVED EXCITATION
(a)
REMOVE DICKMAN DYNAMICAL MODEL
(c)
REMOVE AAM & OAM
(b)
REMOVE G/S/B DYNAMICAL MODEL
(d)
psd in db (mas^2/cpy)
frequency (cycles/year)
−60.0
−30.0
0.0
30.0
60.0
20.0
10.0

Gross (2008)

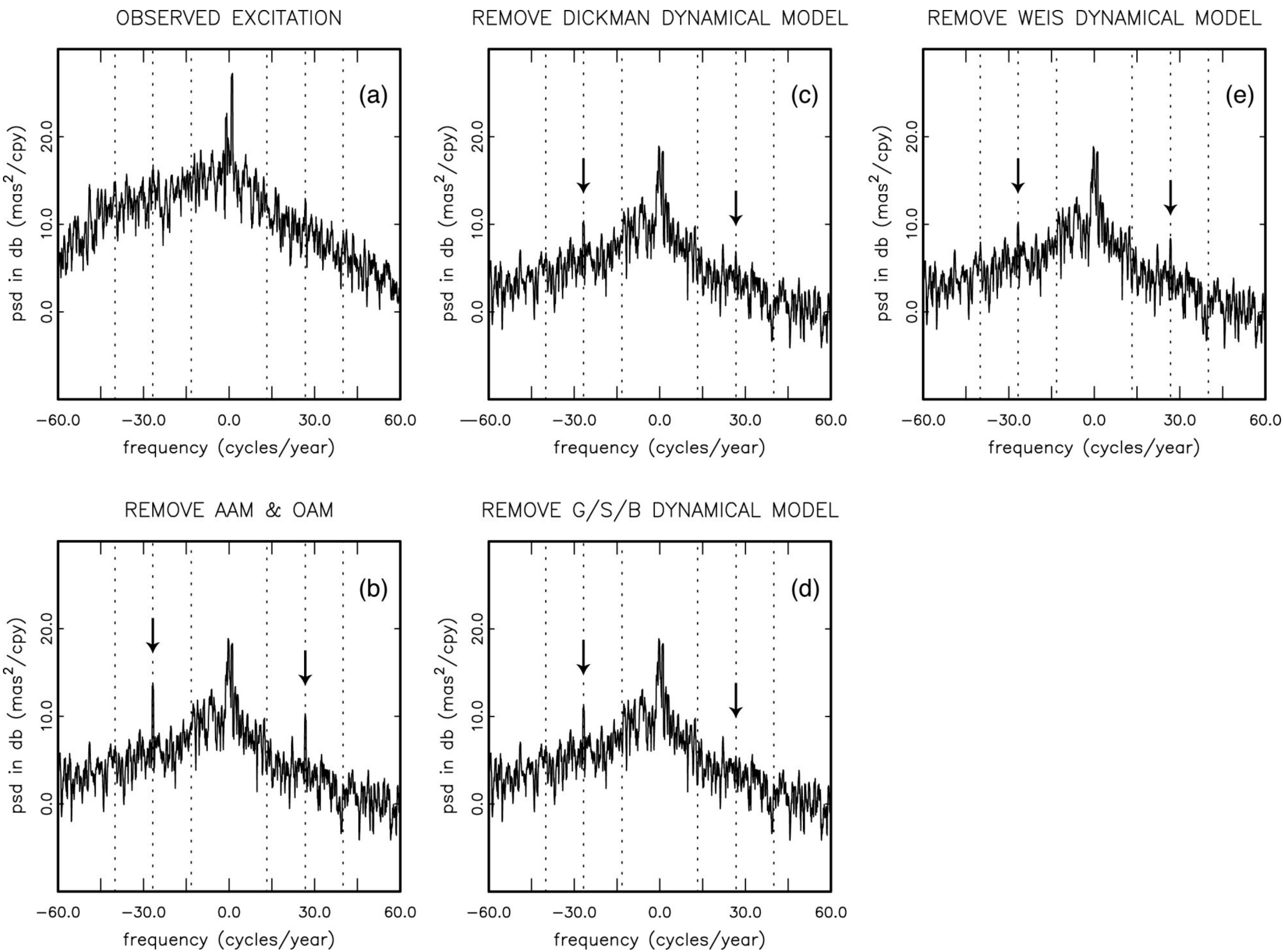
OBSERVED EXCITATION
REMOVE DICKMAN DYNAMICAL MODEL
REMOVE WEIS DYNAMICAL MODEL
REMOVE AAM & OAM
REMOVE G/S/B DYNAMICAL MODEL
(a)
(b)
(c)
(d)
(e)
psd in db (mas^2/cpy)
frequency (cycles/year)
−60.0
−30.0
0.0
30.0
60.0
0.0
10.0
20.0

Gross (2008)

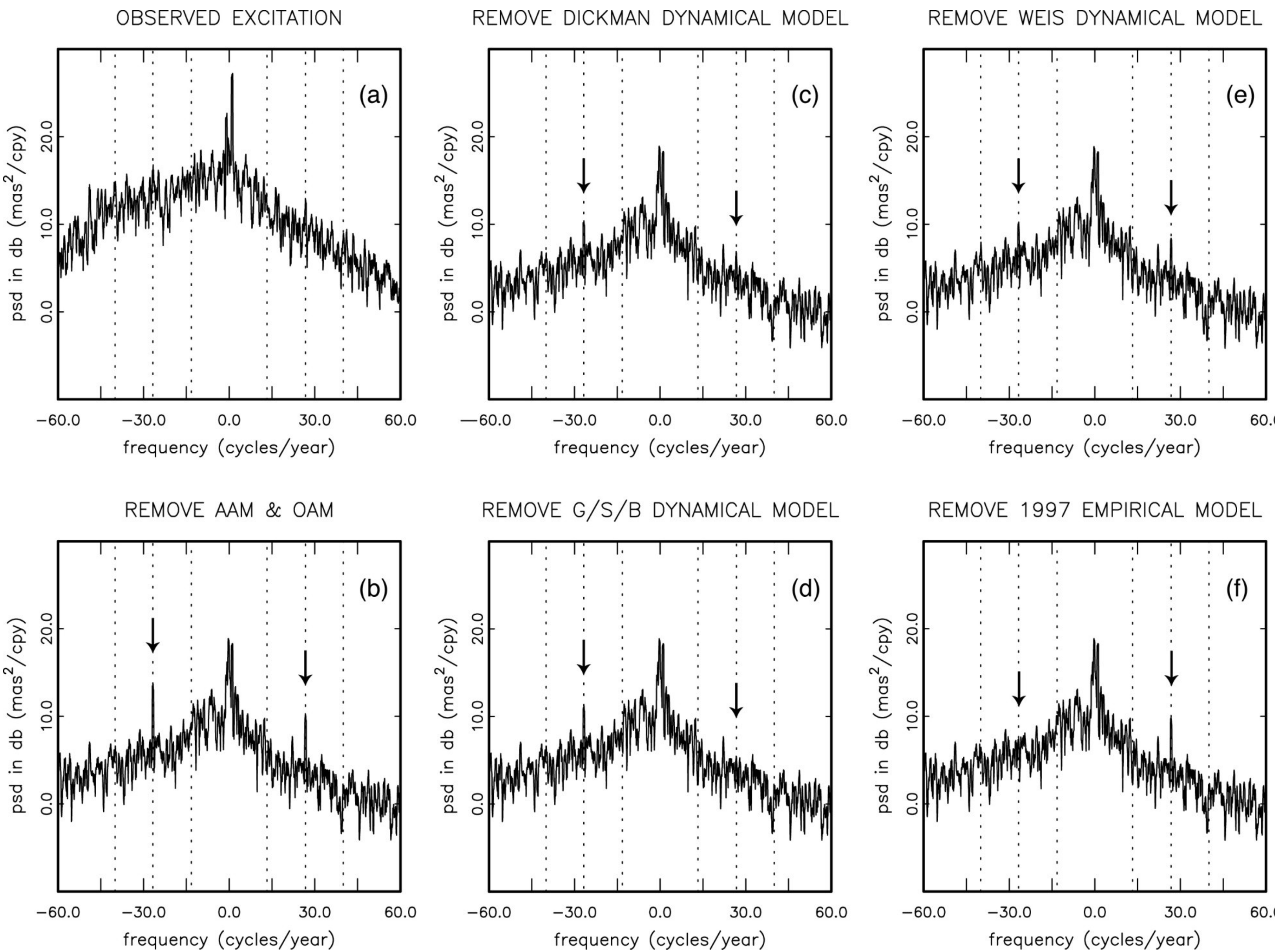

OBSERVED EXCITATION
REMOVE DICKMAN DYNAMICAL MODEL
REMOVE WEIS DYNAMICAL MODEL
REMOVE AAM & OAM
REMOVE G/S/B DYNAMICAL MODEL
REMOVE 1997 EMPIRICAL MODEL
(a)
(b)
(c)
(d)
(e)
(f)
psd in db (mas²/cpy)
0.0
10.0
20.0
frequency (cycles/year)
−60.0
−30.0
0.0
30.0
60.0

Gross (2008)

Remove Dickman & Nam

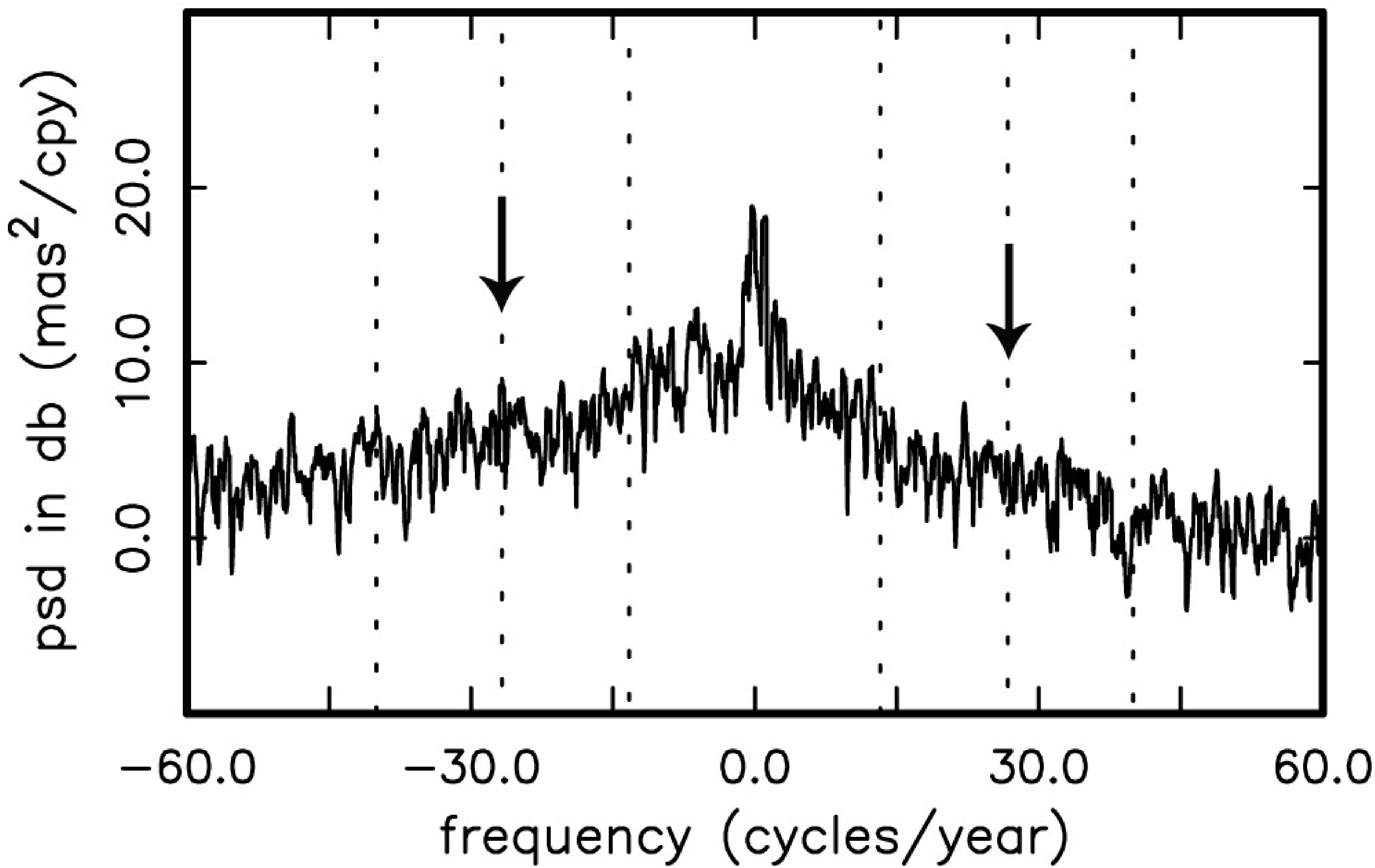

Dickman & Gross (2010)

Tidal Variations: Subdaily

Subdaily Earth Orientation Variations

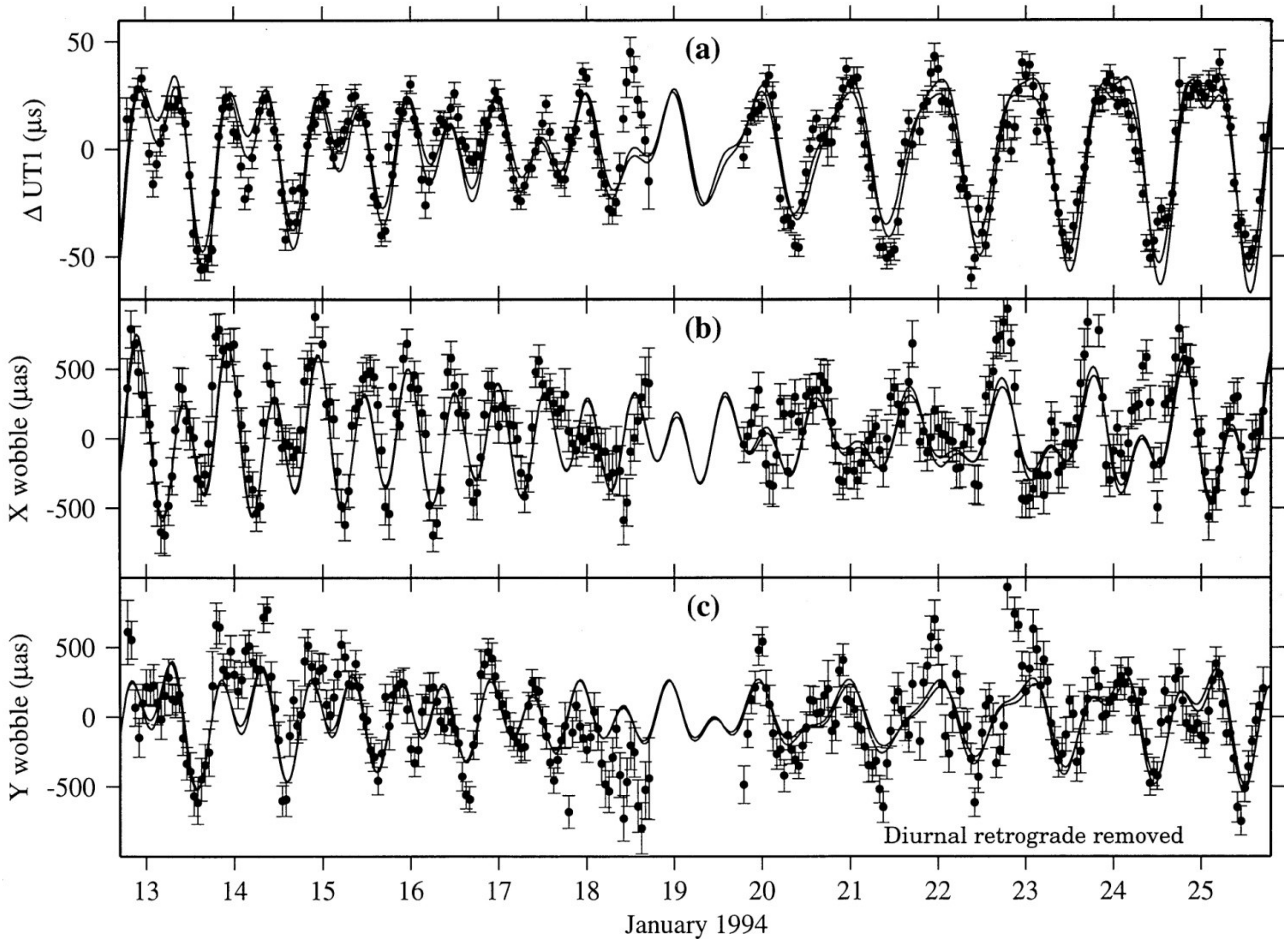

Plots of observed and modeled (a) UT1, (b) *x*-component of polar motion, and (c) *y*-component of polar motion during the Cont94 measurement campaign of January 12–26, 1994. The dots with 1σ error bars are the hourly VLBI observations. Polar motion variations in the retrograde nearly diurnal frequency band have been removed from the observed series and are not included in the modeled series. The solid lines are the predicted effects from the diurnal and semidiurnal T/P ocean tide models B and C of Chao *et al.* (1996). Each tide model explains about 90% of the observed UT1 variance and about 60% of the observed polar motion variance.

Chao et al. (1996)

Non-Tidal Variations: Decadal

Decadal Earth Rotation Variations

- Observed excitation
  - Extended COMB2002
    - Combination of optical astrometric, LLR, SLR, VLBI, and GPS measurements
    - Spans 1948–2002 at daily intervals (UT1 and LOD since 1956)
- Atmospheric excitation
  - NCEP/NCAR reanalysis AAM
    - Sum of wind and i.b. pressure terms
    - Spans 1948 to present at 6-hour intervals
- Oceanic excitation
  - ECCO/JPL 50-year OAM
    - Sum of current and bottom pressure terms
    - Spans 1949–2002 at 10-day intervals
- Detrended & low pass filtered
    - Cutoff period of 6 years

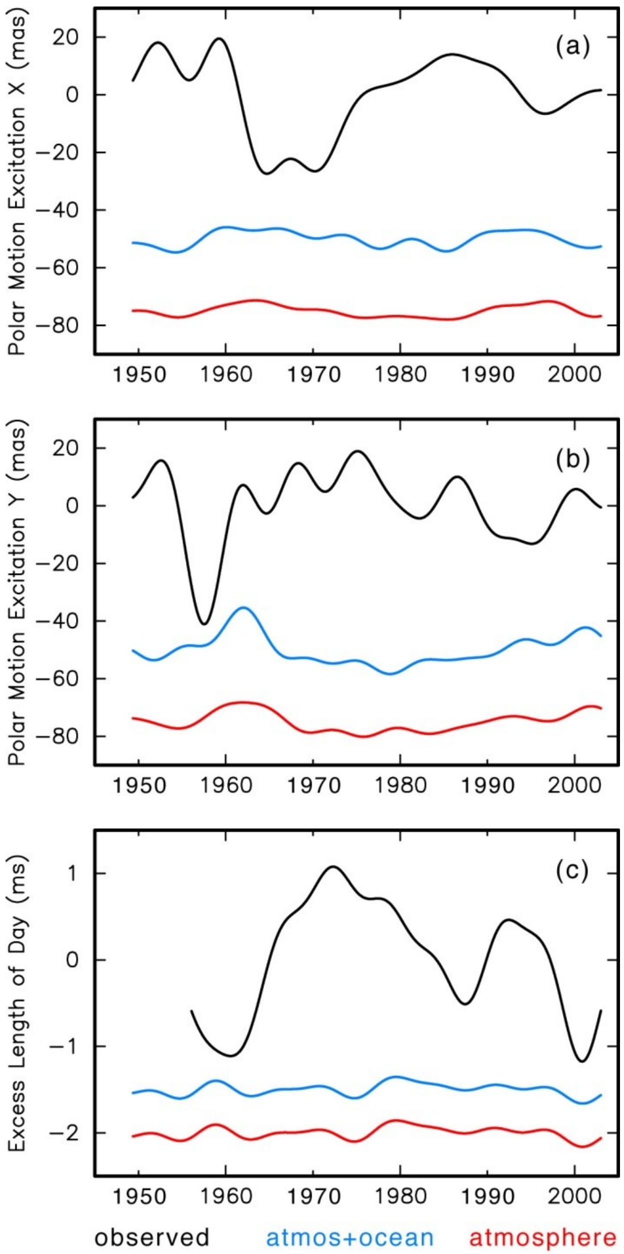

Gross et al. (2005)

Decadal Variations

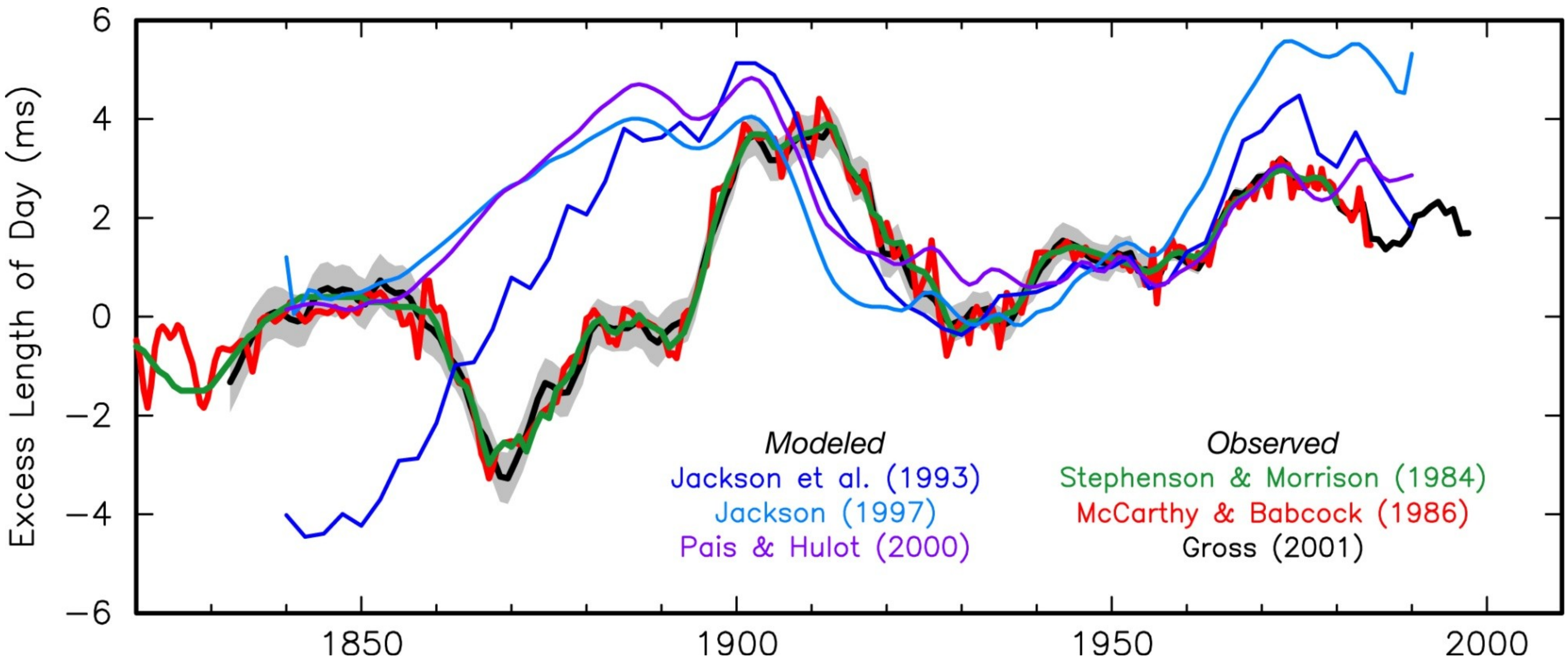

Plots of observed and modeled length-of-day variations on decadal time scales. The observed LOD series are those of Gross (2001; black curve with gray shading representing $\pm$ 1σ standard error), McCarthy and Babcock (1986; red curve), and Stephenson and Morrison (1984; green curve). Note that after about 1955 the uncertainties of the Gross (2001) LOD values are less than the width of the black line. The modeled core angular momentum series are those of Jackson *et al.* (1993; dark blue curve), the *uvm-s* model of Jackson (1997; light blue curve), and the PH-inversion model of Pais and Hulot (2000; purple curve). A secular trend of +1.8 ms/cy has been added to the modeled core angular momentum series to match the observed secular trend. An arbitrary bias has also been added to the modeled series in order to facilitate their comparison with the observed series.

Gross (2007)

Non-Tidal Variations: Sub-Decadal

Sub-Decadal Variations

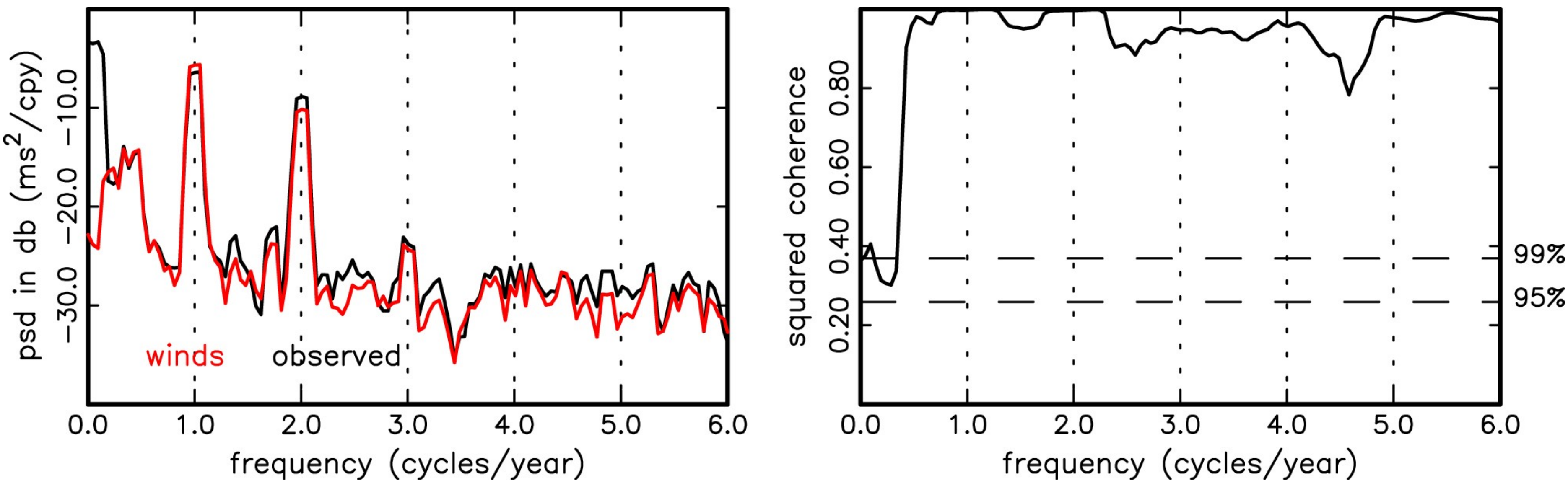

Power spectra (left panel) and squared magnitude of the coherence (right panel) of the observed length-of-day variations during 1980–2000 and those due to atmospheric winds below 10 hPa. The power spectral density (psd) estimates in the left panel, given in decibels (db), were computed by the multitaper method with the spectrum of the observed variations shown in black and that due to the winds shown in red. The horizontal dashed lines in the right panel indicate the 95% and 99% confidence levels of the squared magnitude of the coherence between the observed and wind-driven LOD variations.

Gross et al. (2004)

Seasonal Variations

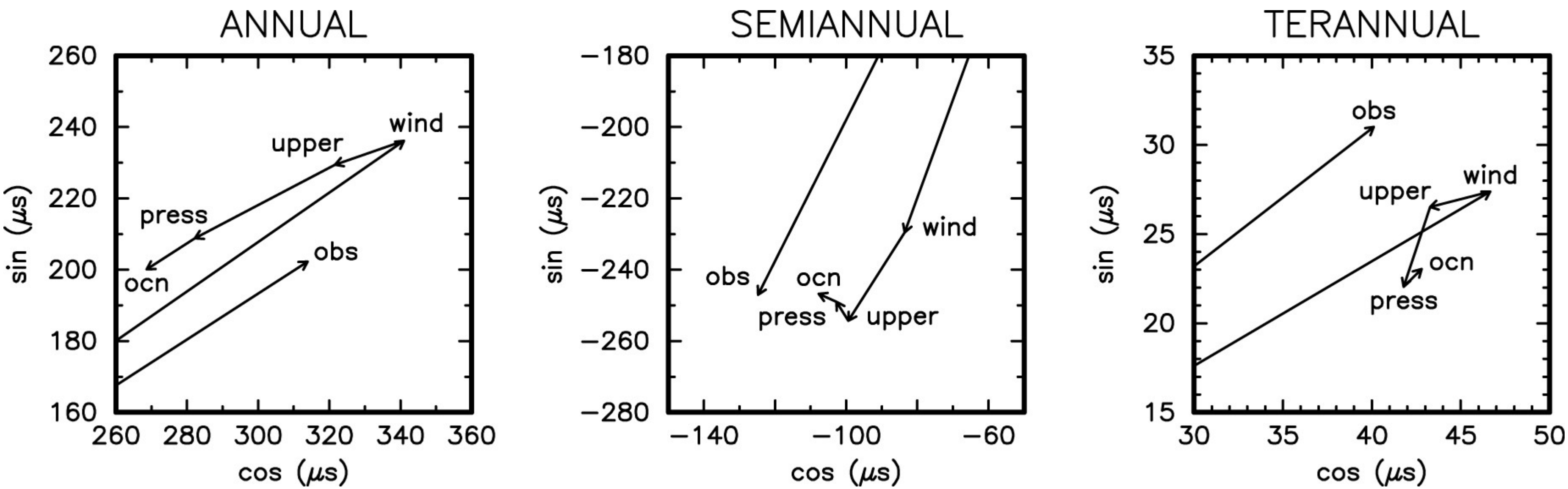

Phasor diagrams of the annual (left panel), semiannual (middle panel), and terannual (right panel) components of the observed length-of-day variations (obs) during 1992–2000 and of the effects on the LOD during this time period of atmospheric winds below 10 hPa (wind), winds above 10 hPa (upper), surface pressure (press), and the oceans (ocn). The atmospheric surface pressure term was computed by assuming that the oceans respond as an inverted barometer to the imposed surface pressure variations. The oceanic results include the effects of both currents and ocean-bottom pressure. The reference date for the phase is January 1.0, 1990 which in the diagram is measured counterclockwise starting from a horizontal position. Note the change in scale of the terannual phasor diagram.

Gross et al. (2004)

Intraseasonal Variations

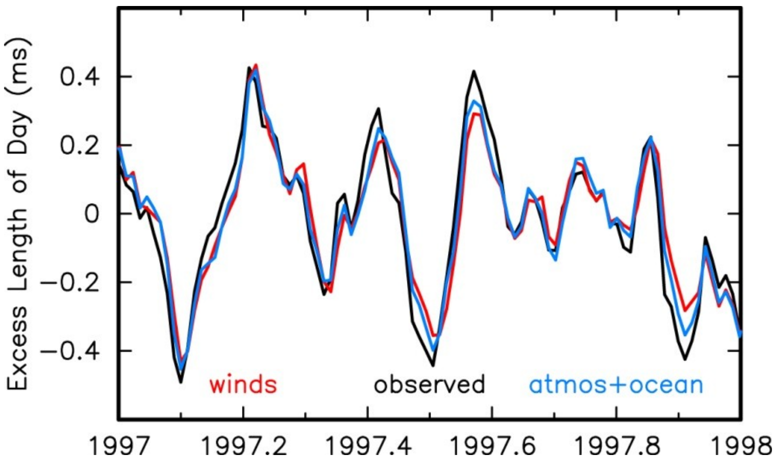

Observed length-of-day variations (black); variations caused by the modeled atmospheric winds (red); and variations caused by the sum of the modeled atmospheric winds, surface pressure, oceanic currents, and bottom pressure (blue) on intraseasonal time scales during 1997. Intraseasonal variations considered here have periods ranging between 4 days and 1 year excluding signals at the annual, semiannual, and terannual frequencies. The atmospheric surface pressure term is that computed assuming the oceans respond as an inverted barometer to the imposed surface pressure variations. The contribution to intraseasonal LOD variations of the winds between 10 hPa and 0.3 hPa is included in the red and blue curves. The mean has been removed from all series.

Excitation process	Variance explained	Correlation
Atmospheric		
winds (ground to 10 hPa)	85.8%	0.93
winds (10 hPa to 0.3 hPa)	1.1%	0.12
all winds (ground to 0.3 hPa)	85.9%	0.93
surface pressure (i.b.)	3.3%	0.18
all winds and surface pressure (i.b.)	90.2%	0.95
Oceanic		
currents	4.1%	0.36
bottom pressure	3.3%	0.30
currents and bottom pressure	7.0%	0.36
Atmospheric and oceanic		
all winds and currents	87.4%	0.94
surface (i.b.) and bottom pressure	5.9%	0.25
Total of all atmospheric and oceanic		
w/o winds above 10 hPa	91.9%	0.96
with winds above 10 hPa	92.2%	0.96

%, percentage; i.b., inverted barometer; w/o, without; 99% significance level for correlations is 0.18; intraseasonal variations considered here have periods ranging between 4 days and 1 year excluding signals at the annual, semiannual, and terannual frequencies

Gross et al. (2004)

Interannual Variations

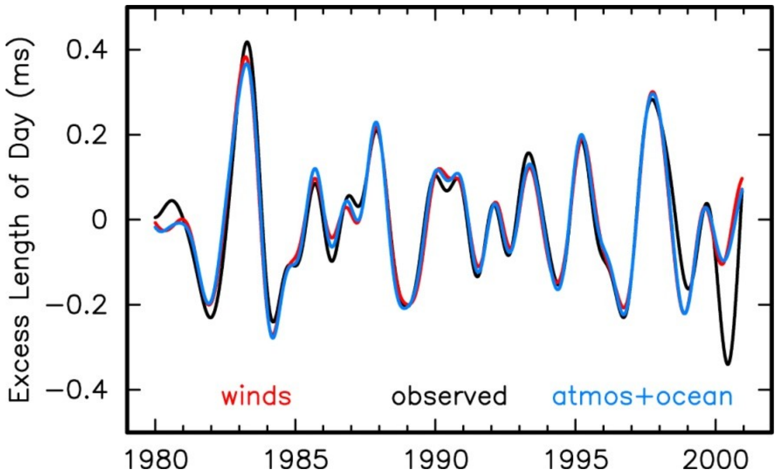

Observed length-of-day variations (black); variations caused by the modeled atmospheric winds (red); and variations caused by the sum of the modeled atmospheric winds, surface pressure, oceanic currents, and ocean-bottom pressure (blue) on interannual time scales during 1980–2000. The interannual frequency band ranges from 1/5 cpy to 1 cpy. The atmospheric surface pressure term is that computed assuming the oceans respond as an inverted barometer to the imposed surface pressure variations. The mean has been removed from all series.

Excitation process	Variance explained	Correlation
Atmospheric		
winds (ground to 10 hPa)	85.8%	0.93
surface pressure (i.b.)	2.6%	0.24
winds and surface pressure (i.b.)	87.3%	0.93
Oceanic		
currents	0.6%	0.14
bottom pressure	0.4%	0.09
currents and bottom pressure	0.8%	0.12
Atmospheric and oceanic		
winds and currents	86.2%	0.93
surface (i.b.) and bottom pressure	2.9%	0.23
Total of all atmospheric and oceanic	87.9%	0.94

%, percentage; i.b., inverted barometer; 99% significance level for correlations is 0.38; interannual frequency band ranges from 1/5 cpy to 1 cpy

Gross et al. (2004)

POLAR MOTION EXCITATION

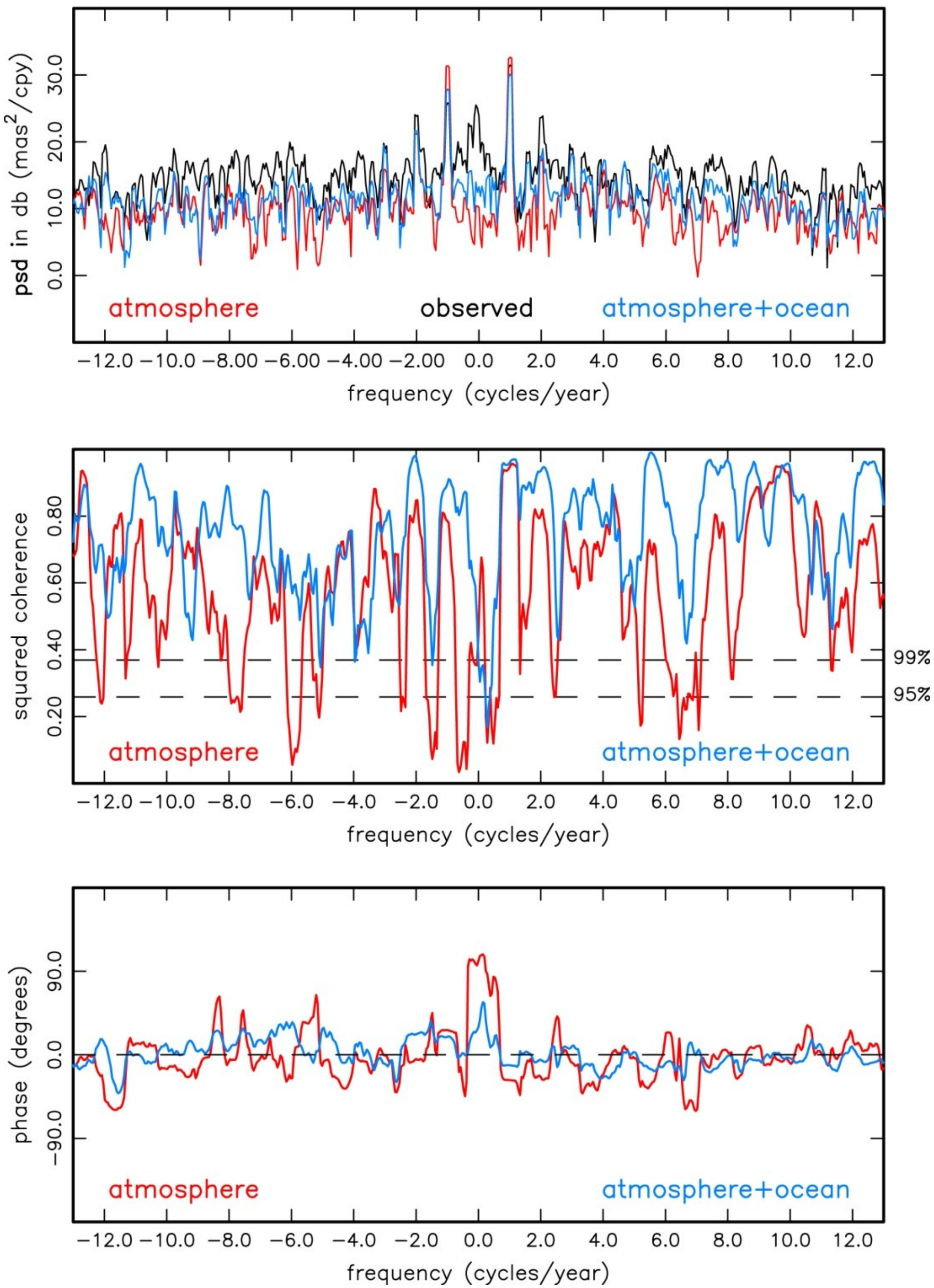

Gross (2005)

Summary

Mass Transport in the Earth System

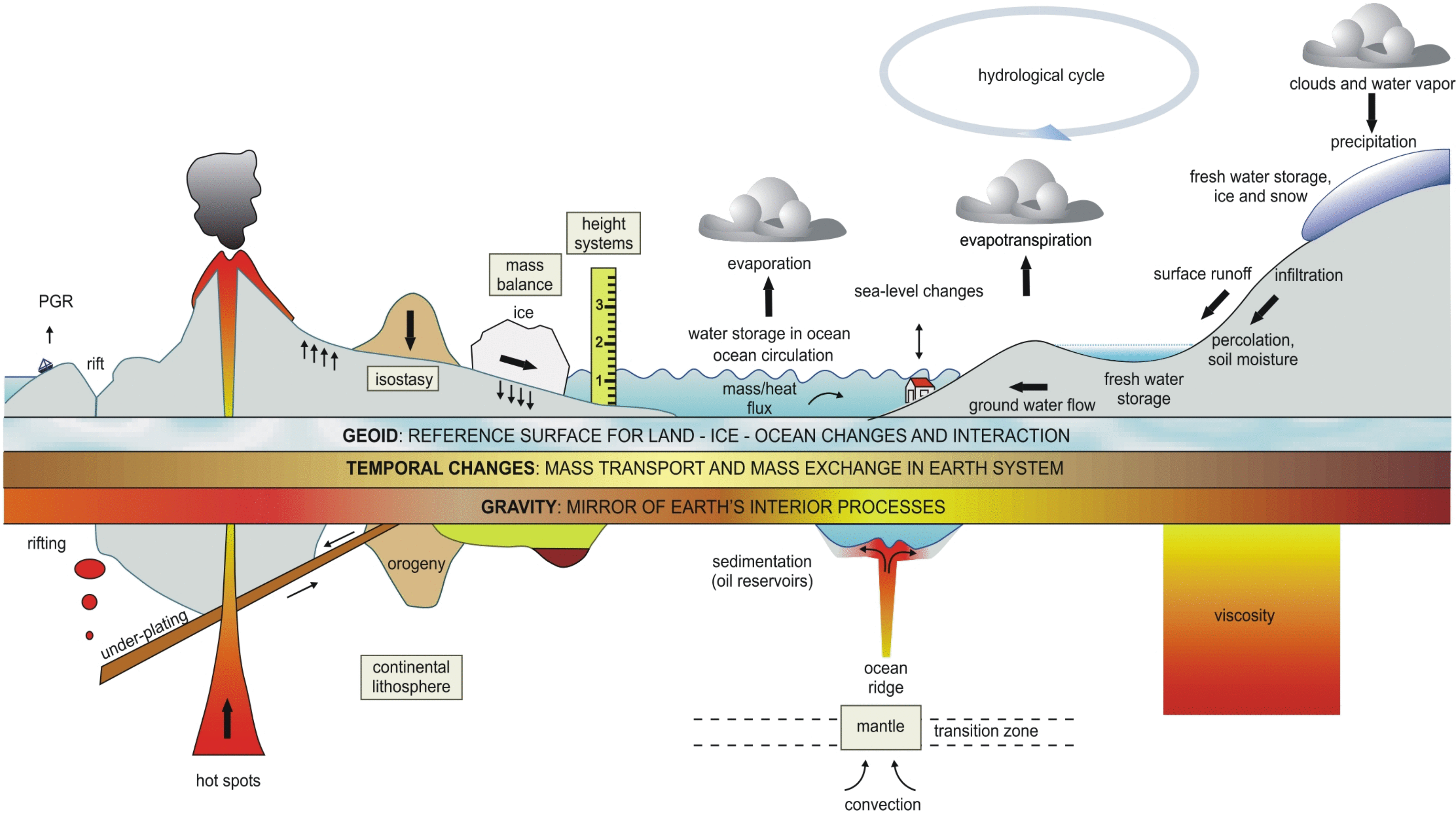

Ilk et al. (2005)

Forcing Mechanisms

- External
  - Tidal potential
    - Body, ocean, atmosphere
- Surficial
  - Atmospheric winds and surface pressure
  - Oceanic currents and bottom pressure
  - Water stored on land (liquid, snow, ice)
- Internal
  - Earthquakes and tectonic motions
  - Mantle convection
  - Outer core dynamics / coupling with mantle
  - Inner core dynamics / coupling with outer core and mantle

Geodetic Measures of Earth's Response

- Rotation
  - Angular momentum exchange (surface fluids, outer core)
  - Torques (external, surficial, internal)
  - Changes in inertia tensor (earthquakes, GIA)
- Gravity and geocenter
  - Mass distribution (static field)
  - Mass redistribution (time varying field)
  - Surface displacements (ground-based)
- Shape
  - Tidal displacements
  - Surface loading and unloading
  - Internal deformation
    - Earthquakes, core pressure => mantle deformation